Supporting Information for

GTP cyclohydrolase 1/tetrahydrobiopterin counteract ferroptosis through lipid remodeling

Vanessa A.N. Kraft[1,9], Carla T. Bezjian[2,9], Susanne Pfeiffer[1,9], Larissa Ringelstetter[3], Constanze Müller[4], Fereshteh Zandkarimi[5], Juliane Merl-Pham[6], Xuanwen Bao[7], Natasa Anastasov[7], Johanna Kössl[1], Stefanie Brandner[3], Jacob D. Daniels[8], Philippe Schmitt-Kopplin[4], Stefanie M. Hauck[6], Brent R. Stockwell[2,5,*], Kamyar Hadian[3,*], Joel A. Schick[1,*]

[1]Institute for Molecular Toxicology and Pharmacology, Genetics and Cellular Engineering Group, HelmholtzZentrum Muenchen, Ingolstaedter Landstr. 1, 85764 Neuherberg, Germany

[2]Department of Chemistry, Columbia University, 550 West 120th Street, MC4846, New York, NY, 10027, USA

[3]Institute for Molecular Toxicology and Pharmacology, Assay Development and Screening Platform, HelmholtzZentrum Muenchen, Ingolstaedter Landstr. 1, 85764 Neuherberg, Germany

[4]Research Unit Analytical BioGeoChemistry, HelmholtzZentrum Muenchen, Ingolstaedter Landstr. 1, 85764 Neuherberg, Germany

[5]Department of Biological Sciences, Columbia University, New York, NY, 10027, USA

[6]Research Unit Protein Science, HelmholtzZentrum Muenchen, Ingolstaedter Landstr. 1, 85764 Neuherberg, Germany

[7]Institute of Radiation Biology, HelmholtzZentrum Muenchen, Ingolstaedter Landstr. 1, 85764 Neuherberg, Germany

[8]Department of Pharmacology, Columbia University, New York, NY, 10027, USA

[9]These authors contributed equally to this work

*Correspondence: joel.schick@helmholtz-muenchen.de (J.A.S.), kamyar.hadian@helmholtz-muenchen.de (K.H.), bstockwell@columbia.edu (B.R.S.)

Table of Contents

See also supporting files Tables S1-S3

Supporting Figure 1

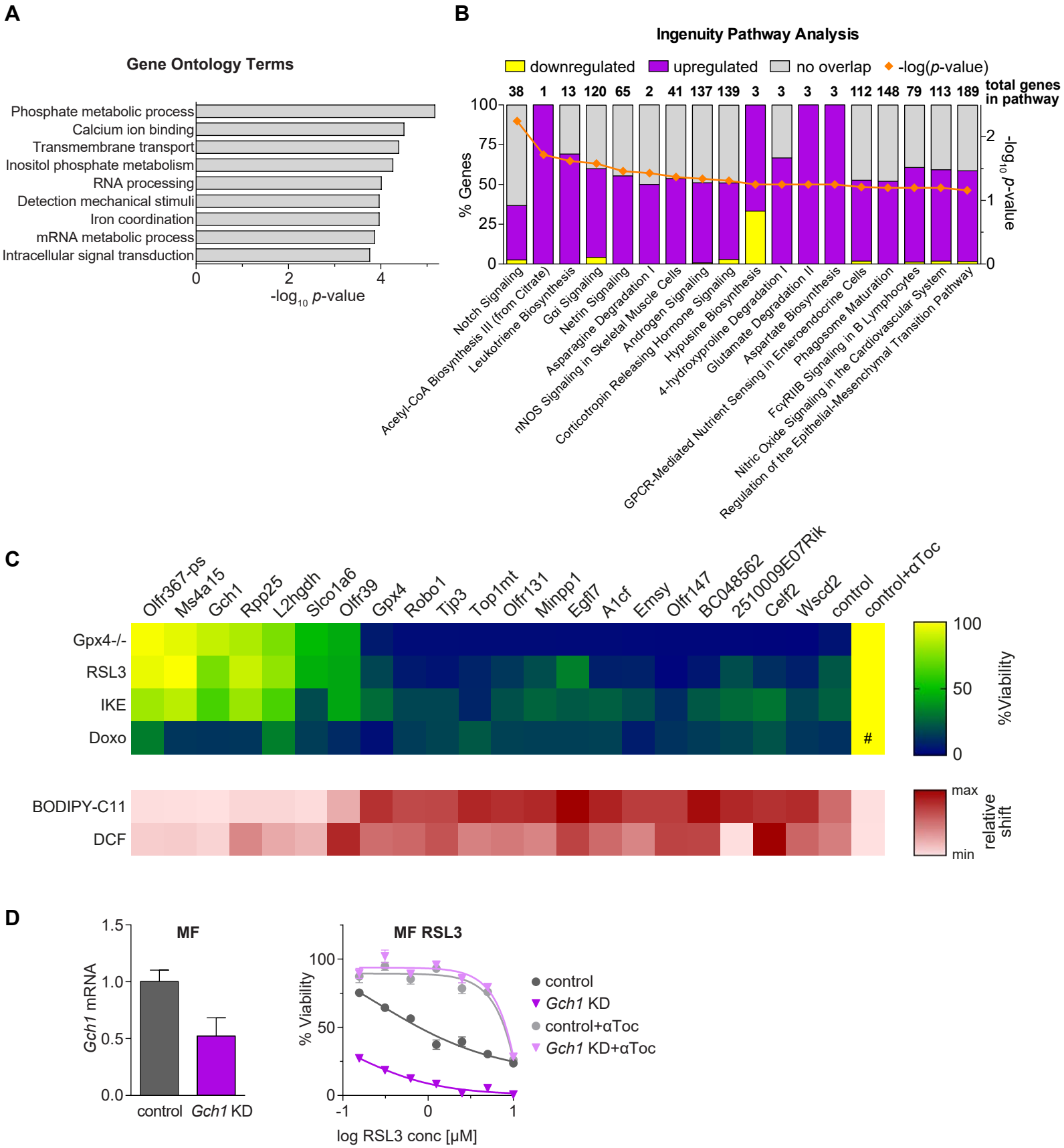

Figure S1. CRISPRa screening results. (A) Gene ontology term integrated analysis of top 30 genes from each treatment. (B) Ingenuity Pathway Analysis of top all genes with $\log_2$ increase > 1.0 and FDR (Bonferroni) corrected *p*-values > 0.05 from each treatment. (C) Heat map validating 21 overexpressing MF cell lines against challenges *Gpx4-/-*, 0.3 μM RSL3, 2 μM IKE and 20 μM doxorubicin (Doxo) compared to empty vector control cells (control): BODIPY 581/591 C11 (BODIPY-C11) and 2,7-Dichlorodihydrofluorescein diacetate (DCF) indicate lipid and cytosolic ROS respectively in these lines after 0.3μM RSL3 treatment for 2 h. Untreated cells (#) serve as control treatment for Doxo. (D) Relative *Gch1* mRNA levels and dose response curve of *Gch1* CRISPRi knockdown MF cells (*Gch1* KD) compared to empty vector control cells (control) against RSL3 with 10 μM α-tocopherol (αToc) rescue. Viability data is plotted as mean ± SEM of n=3 technical replicates of at least three repetitions of the experiment with similar results. Relative mRNA expression is shown as mean ± SD of n=3 technical replicates.

Supporting Figure 2

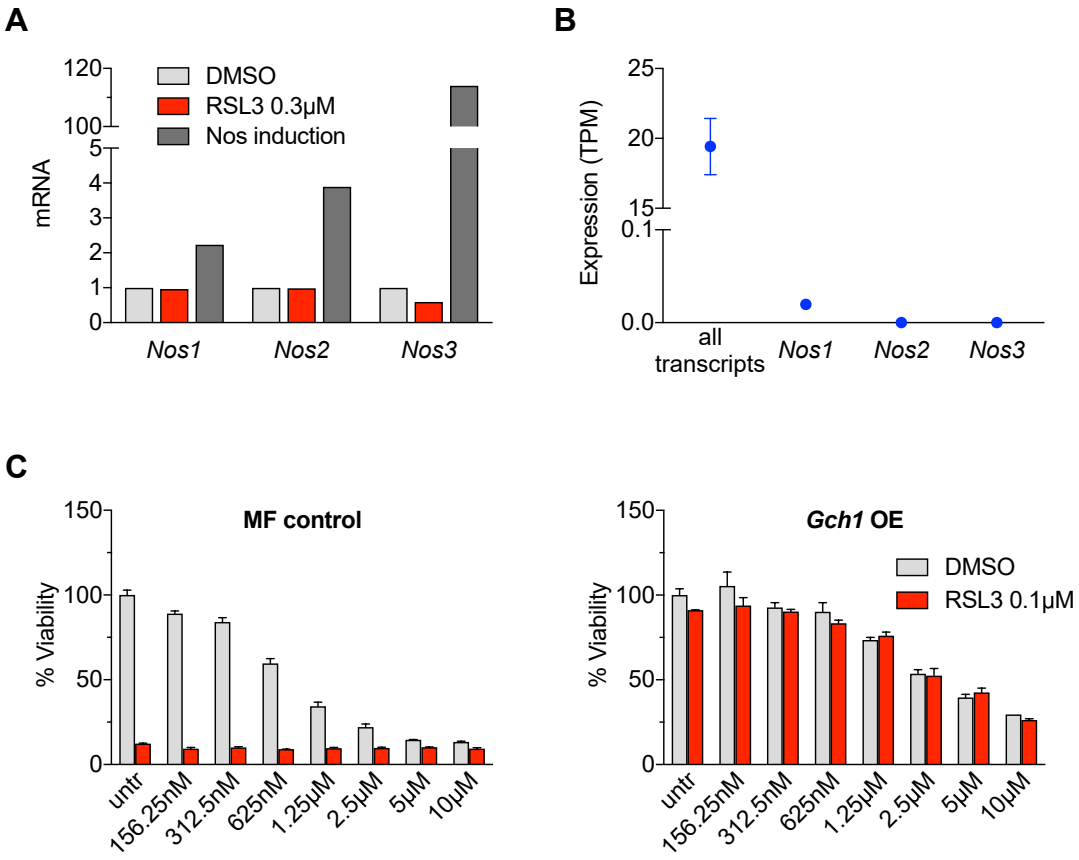

Figure S2. Nitric oxide synthases do not contribute to ferroptosis resistance in *Gch1* OE cells. (A) Expression level of *Nos1*, *Nos2*, and *Nos3* mRNA measured by qPCR after RSL3 and *Nos* inducing control treatment in MF control cells. Induction of *Nos1* by 10 ng/ml TNFα for 14 h, *Nos2* by 5μg/mL lipopolysaccharide (LPS). *Nos3* positive control was detected in murine cDNA. Relative mRNA expression is shown as mean ± SD of n=3 technical replicates. (B) Expression level of *Nos1*, *Nos2*, and *Nos3* measured by deep sequencing in parental MF cells. (C) Effect of diphenyleneiodonium chloride (DPI) on MF control and *Gch1* OE cells induced by 0.1 μM RSL3. Viability data is plotted as mean ± SEM of n=3 technical replicates of at least three repetitions of the experiment with similar outcomes.

Supporting Figure 3

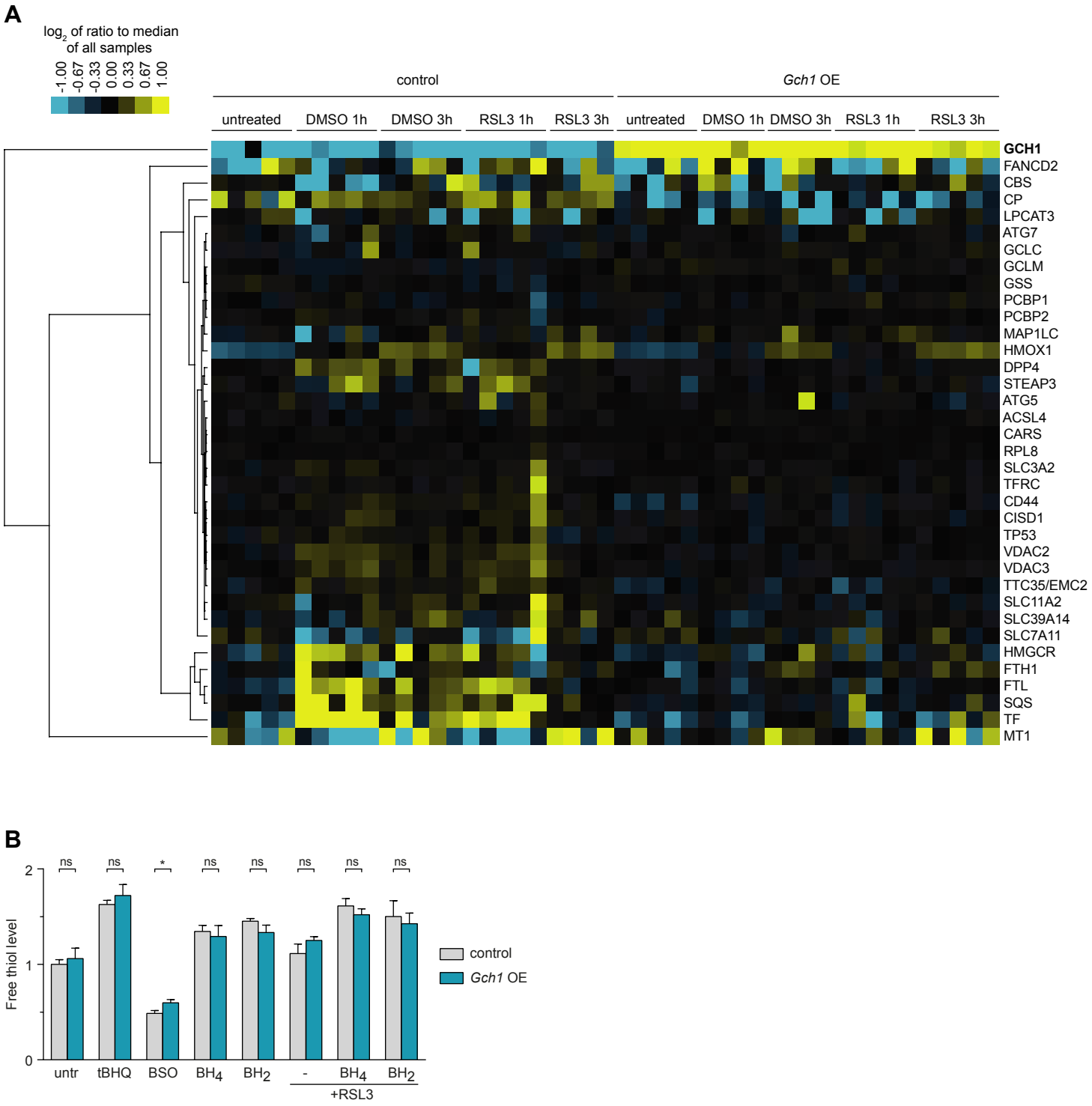

Figure S3. GCH1 overexpression does not affect known ferroptosis regulators. (A) Protein levels of known ferroptosis regulators upon 1 h and 3 h 0.3 µM RSL3 and DMSO treatment in *Gch1* overexpressing MF cells (*Gch1* OE) cells compared to empty vector control cells (control). Each column represents one of n=4 or 5 independent biological replicates. (B) Free thiol levels in *Gch1* OE cells compared to MF control cells treated with 25 µM tert-butylhydroquinone (tBHQ), 100 µM buthionine sulfoximine (BSO), 25 µM BH_4 and BH_2 and ferroptosis induction by 0.3 µM RLS3. Data are shown as mean ± SD of n=3 technical replicates of three independent repetitions of the experiment with similar results.

Supporting Figure 4

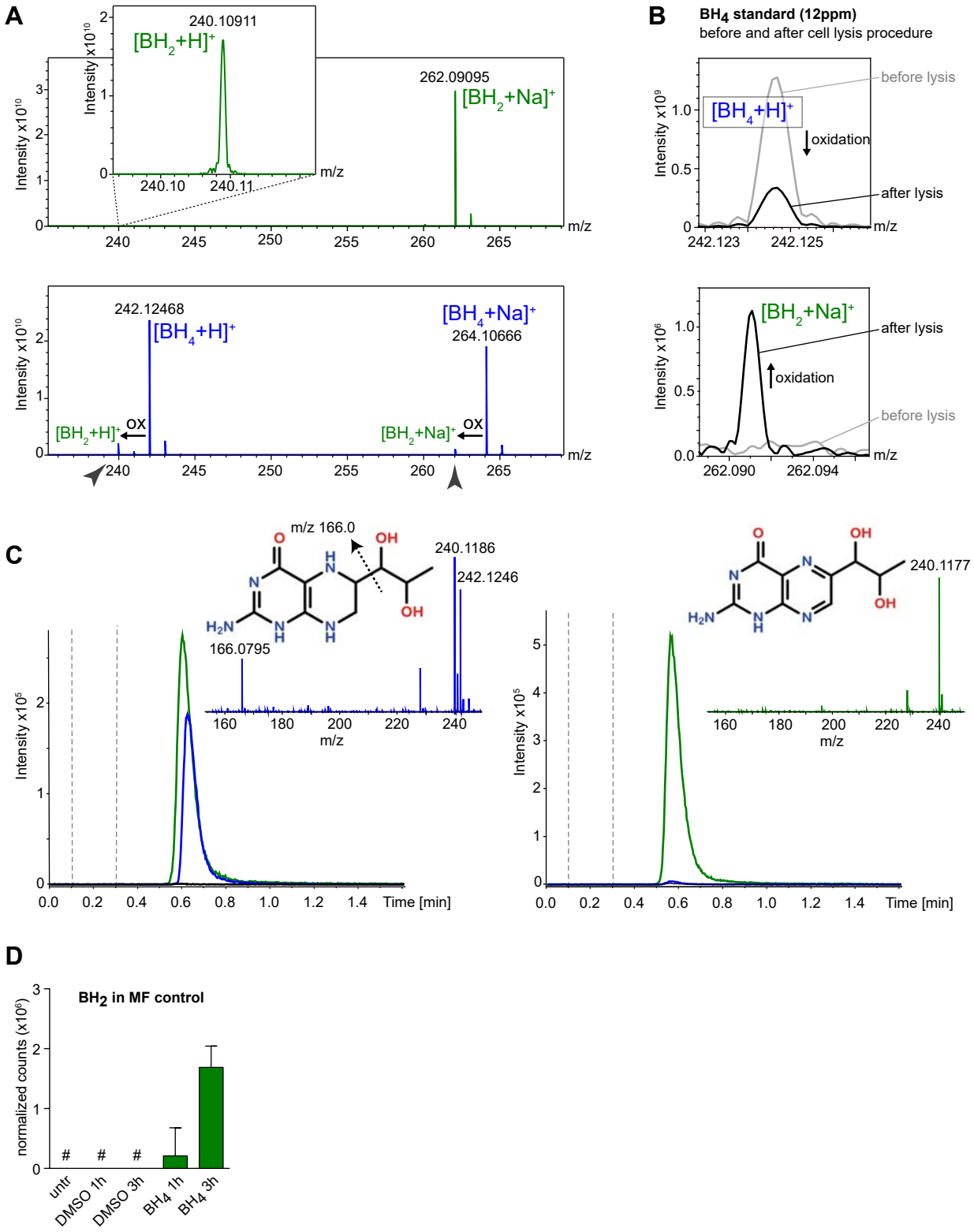

Figure S4. Oxidation of BH_4 into BH_2 and Identification of enhanced presence of BH_4 using targeted LC-MS². (A) FT/ICR-MS spectra of pure and freshly prepared standards showed an in-source auto-oxidation of BH_4 into BH_2 during direct injection MS analysis (ESI capillary voltage = 3.5 kV). FT/ICR-MS spectra (50scans) for BH_4 standard 12 ppm (blue) and BH_2 standard (green). (B) Effect of bead-based cell preparation using soft conditions (2x30sec, -4°C) 12 ppm BH_4 standard before and after cell lysis in the m/z range of 242.123 - 242.127 (BH_4+H^+) and 262.090 to 262.094 (BH_2+Na^+), 5 scans. Abbreviation: ox, oxidation. (C) UPLC-ToF-MS/MS targeted analysis for identification of BH_4 and BH_2 with exact mass, main fragmentation pattern and retention time. (D) Delayed emergence of BH_2 in MF control cells after treatment with BH_4. Data is shown as mean ± SD of five biological replicates.

Supporting Figure 5

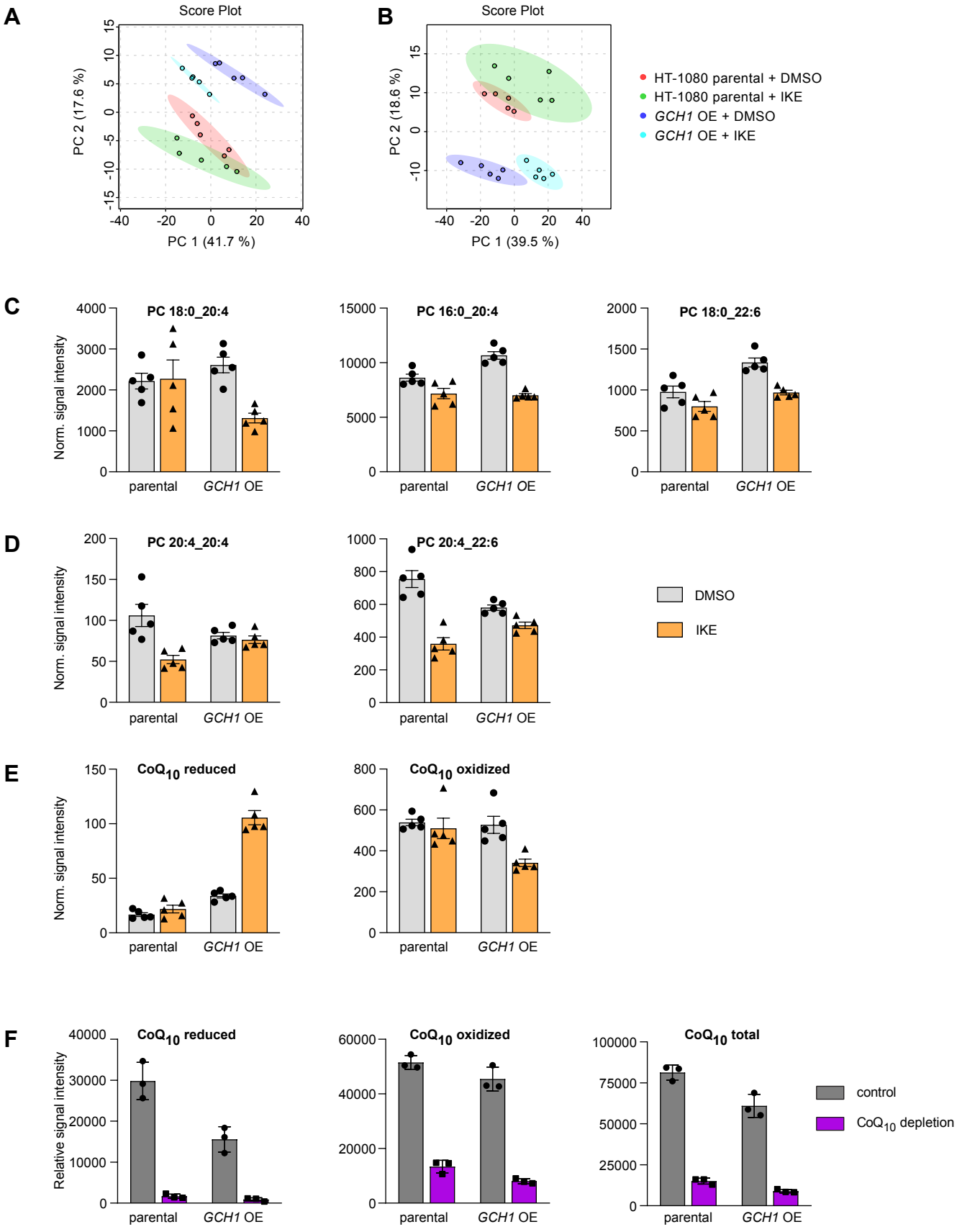

Figure S5. Lipidomic analysis of *GCH1*-overexpressing (*GCH1* OE) compared to parental HT-1080 cells. (A-B) Unsupervised Principal Component Analysis (PCA score plot) of extracted lipid features in both positive (A) and negative (B) electrospray ionization modes. (C-F) Relative normalized signal intensities of phosphatidylcholines (PCs) and coenzyme Q_{10} (CoQ_{10}) in *GCH1* OE compared to parental HT-1080 cells. Untargeted mass spectrometry-based lipidomic detection of (C) one-tailed PUFAs: PC 18:0_20:4, PC 16:0_20:4, PC 18:0_22:6; (D) two-tailed PUFAs: PC 20:4_20:4, PC 20:4_22:6; (E) reduced CoQ_{10} and oxidized CoQ_{10}. Data is shown as mean ± SEM of n=5 independent biological samples. (F) Validation of decreased CoQ_{10} levels upon CoQ_{10} depletion measured using UPLC-MS. Data is shown as mean ± SD of n=3 independent biological samples.

Supporting Figure 6

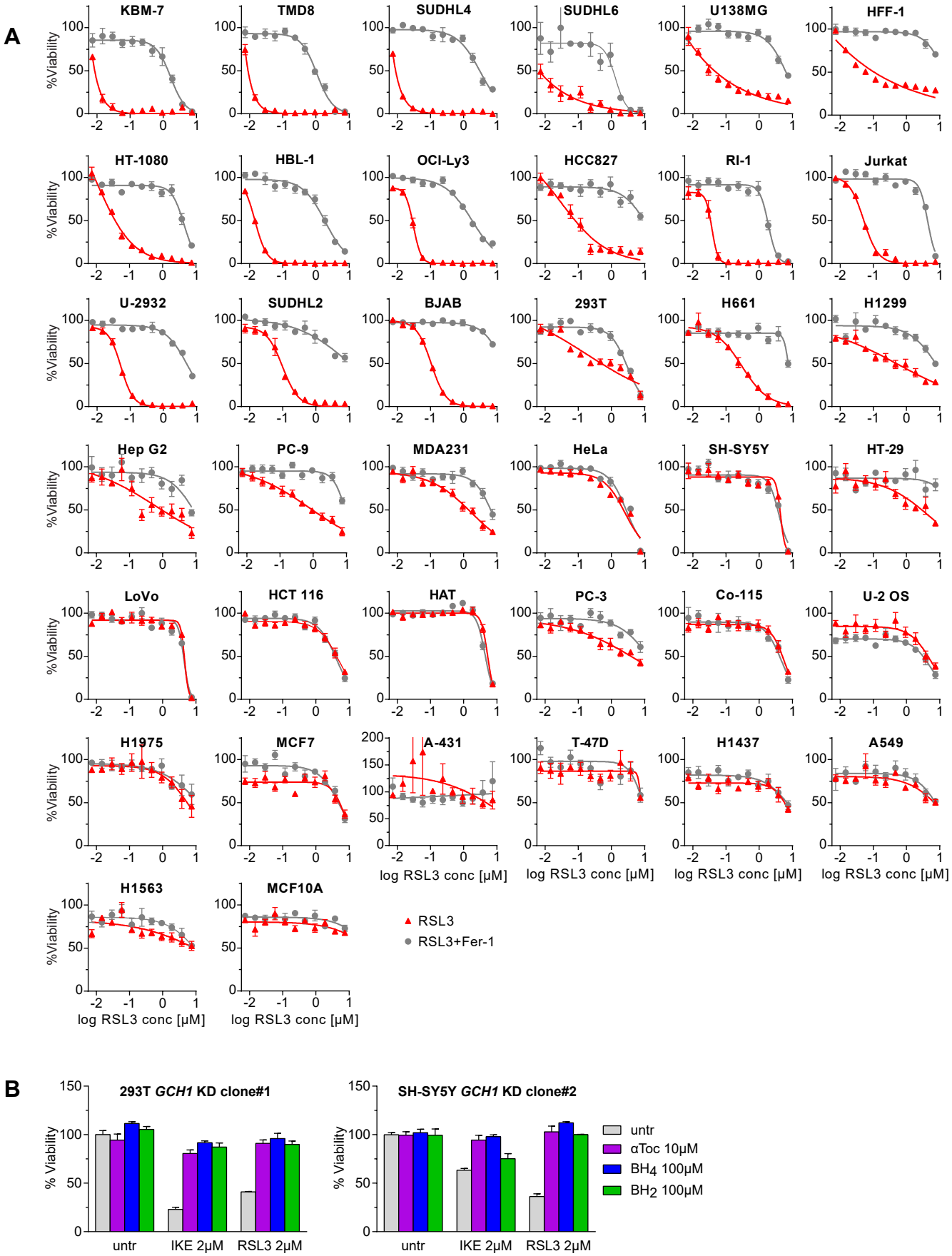

Figure S6. GCH1 expression level determines cancer cell resistance to ferroptosis. (A) Dose response curve panel of 38 cancer cell lines against RSL3 with 2 µM ferrostatin-1 (Fer-1) rescue control. (B) Rescue of *GCH1* knockdown (*GCH1* KD) in 293T and SH-SY5Y cells by either 10 µM α-tocopherol (αToc), 100 µM BH_4 or 100 µM BH_2 after induction by 2 µM IKE or 2 µM RSL3. Viability is shown as mean ± SEM of n=4 (A) or n=3 (B) technical replicates.

Supporting Figure 7

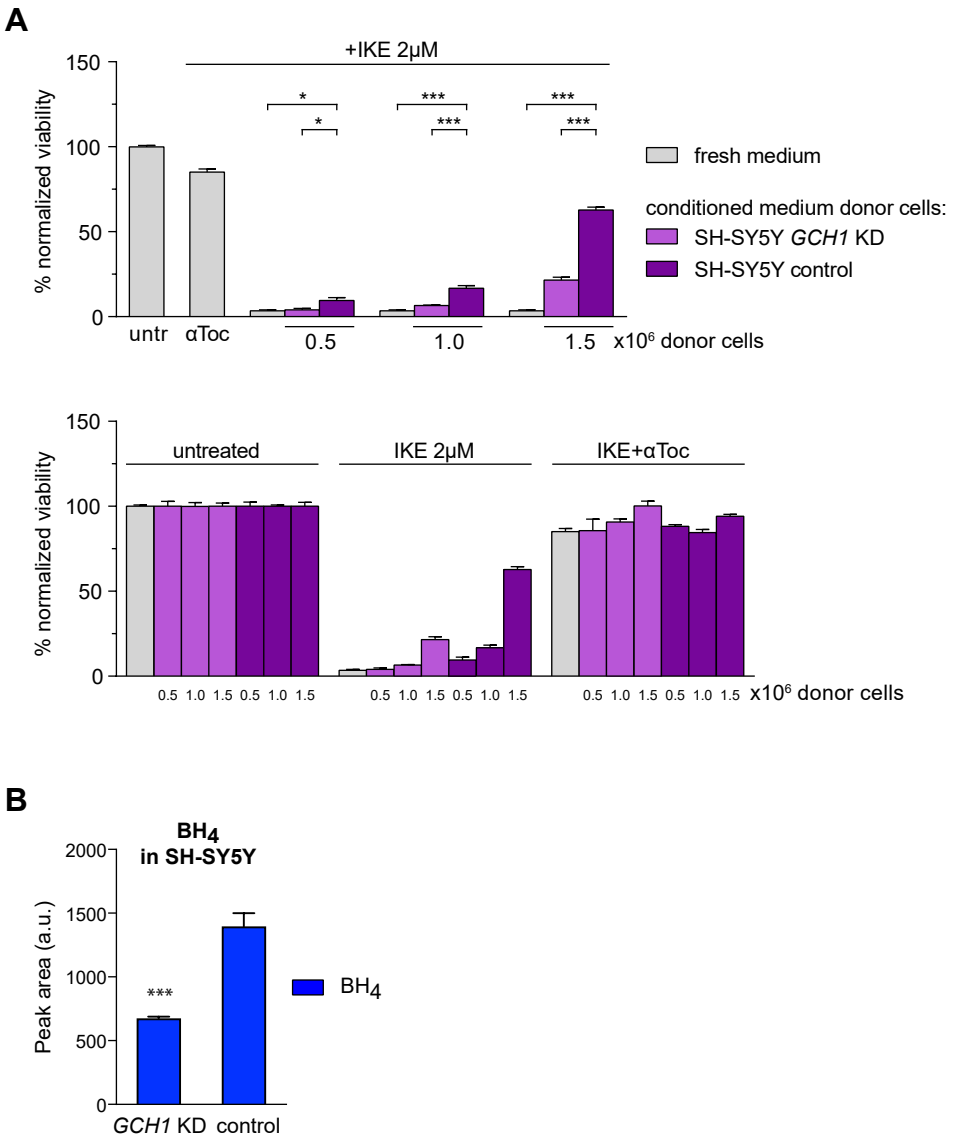

Figure S7. Extrinsic effect of high *GCH1* expressing cells. (A) Effect of conditioned medium from SH-SY5Y control cells (control) compared to SH-SY5Y *GCH1* knockdown (*GCH1* KD) cells. Recipient cells are IKE-induced HT-1080 cells with 10 μM αToc rescue control. The upper panel is an alternative presentation of the same dataset shown in the bottom panel. Viability is reported as mean ± SEM of n=4 technical replicates. A typical result out of four independent experiments is shown. (B) Targeted detection of BH_4 in cell lysates of SH-SY5Y control donor cells compared to *GCH1* KD donor cells. Data shows mean ± SD of n=5 independent biological replicates.

Supporting Figure 8

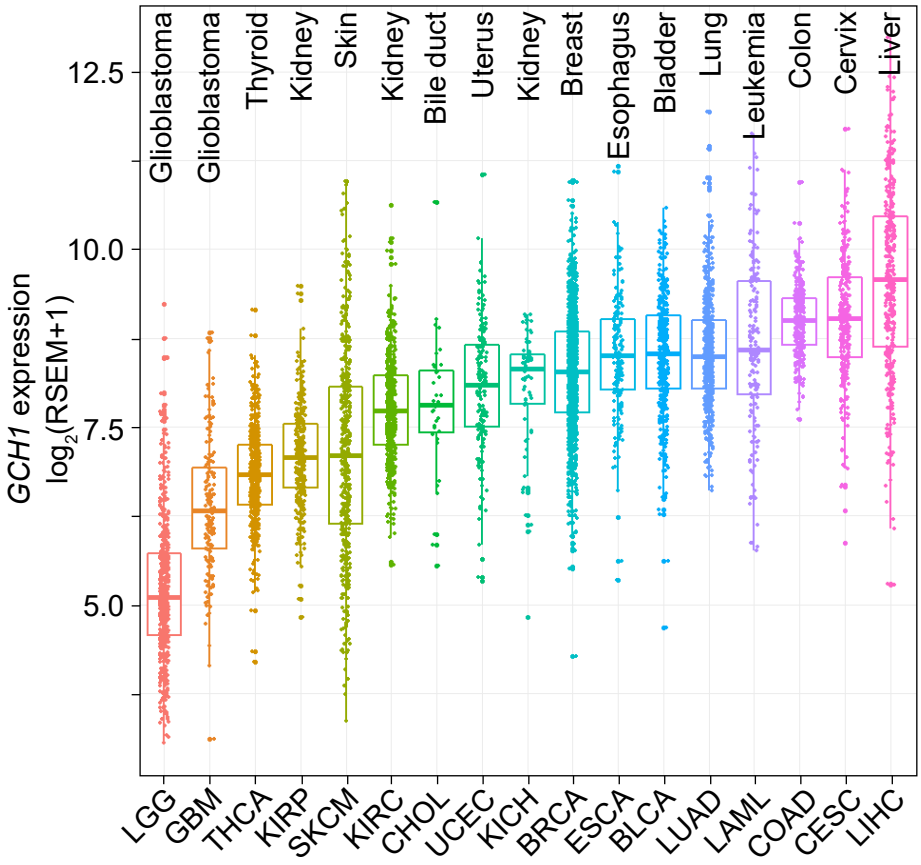

Figure S8. Human patient *GCH1* levels in diverse cancer patients. *GCH1* mRNA expression in human tumors clustered according to tissue of origin.

SUPPORTING TABLES

Table S4. CRISPR guide sequences used in this study. Source [1]

Name	Sequence
Human GCH1 CRISPR guide 1	GCTGTGGCCGGAGTCACCTG
Human GCH1 CRISPR guide 2	GGGCCGGAGTCACCTGAGGA
Human GCH1 CRISPR guide 3	GCAGGTTGCGTACCTTCCTC
Mouse Olfr367-ps CRISPR guide	TAACTGACAGGTCTGGGACT
Mouse Ms4a15 CRISPR guide	AAAGACTGAAGCAAGGGACT
Mouse Gch1 CRISPR guide	TTATGGCAGGGCGACTCGGC
Mouse Rpp25 CRISPR guide	TCCCAAAGGCTGGAGGGACT
Mouse L2hgdh CRISPR guide	CGCCGTGAGTAAGAGGAGCT
Mouse Slco1a6 CRISPR guide	CCTTGAGCGGACCCTGGACT
Mouse Olfr39 CRISPR guide	ATTTCTTTAATGAGGAGCTG
Mouse Gpx4 CRISPR guide	CCAATGGGAAGCCTGAATGA
Mouse Robo1 CRISPR guide	AATATTTCCATCCACATGCC
Mouse Tjp3 CRISPR guide	GCTCTTCCTCCTTCAAGTCG
Mouse Top1mt CRISPR guide	CGGGACTCCTGGACGTGTGG
Mouse Olfr131 CRISPR guide	ATCTCGTGCAATAAAGAAAC
Mouse Minpp1 CRISPR guide	CTCCGACGAGCGTGTGACAC
Mouse Egfl7 CRISPR guide	GGATCCGTCAGCGAACAAAC
Mouse A1cf CRISPR guide	GACCCAATTACCTGGTCAAA
Mouse Emsy CRISPR guide	GTCCGCCCTTTCCTTTCAAA
Mouse Olfr147 CRISPR guide	CTCTATTTCAGTGATGGCTC
Mouse BC048562 CRISPR guide	TGACTGCACAATGCTGCTGT
Mouse 2510009E07Rik CRISPR guide	ATGTGTGCTGACTGTCCTAT
Mouse Celf2 CRISPR guide	AAGGGCTCCTGCAGACTCAC
Mouse Wscd2 CRISPR guide	GGTCCTGTGCAACCTCAAGG

Table S5. Primer sequences used in this study.

Name	Sequence
Human GCH1 amplification forward primer	TTGGCAAAGAATTCGCCACCATGGAGAAGGGCCCTGTGCGGG
Human GCH1 amplification reverse primer	GCTACCTAGCTAGCCTAGCTCCTAATGAGAGTCAGGAACTC
Human GCH1 qPCR forward primer	GCTGTAGCAATCACGGAAGC
Human GCH1 qPCR reverse primer	CACCTCGCATTACCATACACA
Human SLC7A11 qPCR forward primer	GGTGGTGTGTTTGCTGTC
Human SLC7A11 qPCR reverse primer	GCTGGTAGAGGAGTGTGC
Human RPL27 qPCR forward primer	TCGCCAAGAGATCAAAGATAA
Human RPL27 qPCR reverse primer	CTGAAGACATCCTTATTGACG
Human TBP qPCR forward primer	GCGGTTTGCTGCGGTAATC
Human TBP qPCR reverse primer	CTTCACTCTTGGCTCCTGTGC
Mouse Actin qPCR forward primer	CCTCTATGCCAACACAGTGC
Mouse Actin qPCR reverse primer	GTACTCCTGCTTGCTGATCC
Mouse Gapdh qPCR forward primer	GGGTTCCTATAAATACGGACTGC
Mouse Gapdh qPCR reverse primer	CCATTTTGTCTACGGGACGA
Mouse Gch1 qPCR forward primer	GCCTCACCAAACAGATTGC
Mouse Gch1 qPCR reverse primer	CACGCCTCGCATTACCAT
Mouse Nos1 qPCR forward primer	AGATGAGGCACCCCAACTC
Mouse Nos1 qPCR reverse primer	CCTTTACGGGGAAAGAAACG
Mouse Nos2 qPCR forward primer	GAAGGTCGCCAGTCGTGT
Mouse Nos2 qPCR reverse primer	GGAGCCATTTTGGTGACTCTT
Mouse Nos3 qPCR forward primer	ATCCAGTGCCCTGCTTCA
Mouse Nos3 qPCR reverse primer	GCAGGGCAAGTTAGGATCAG

Name	Sequence
Library amplification primer	CCATCTCATCCCTGCGTGTCTCCGACTCAGCTAAGGTAACGGCTTTATATATCTTGTGGAAAGGACG
Library amplification primer	CCATCTCATCCCTGCGTGTCTCCGACTCAGTAAGGAGAACGGCTTTATATATCTTGTGGAAAGGACG
Library amplification primer	CCATCTCATCCCTGCGTGTCTCCGACTCAGAAGAGGATTCGGCTTTATATATCTTGTGGAAAGGACG
Library amplification primer	CCATCTCATCCCTGCGTGTCTCCGACTCAGTACCAAGATCGGCTTTATATATCTTGTGGAAAGGACG
Library amplification primer	CCATCTCATCCCTGCGTGTCTCCGACTCAGCAGAAGGAACGGCTTTATATATCTTGTGGAAAGGACG
Library amplification primer	CCATCTCATCCCTGCGTGTCTCCGACTCAGCTGCAAGTTCGGCTTTATATATCTTGTGGAAAGGACG
Library sequencing primer	CCTCTCTATGGGCAGTCGGTGATCTGCAGACATGGGTGATCCTCAT

SUPPORTING METHODS

No unexpected or unusually high safety hazards were encountered.

Cell lines and culture conditions

All cell lines were grown in their preferred medium supplemented with 1% L-Glutamine (Thermo Fisher Scientific 25030024) and 1% Penicillin-Streptomycin (Thermo Fisher Scientific 15140122) at 37°C and 5% CO_2. Adherent cells were grown in Dulbecco's Modified Eagle's medium (Thermo Fisher Scientific 21969035) containing 10% fetal bovine serum (Thermo Fisher Scientific 10270106). Suspension cells were grown in RPMI 1640 Medium (Thermo Fisher Scientific 21875034) with 15% serum. HT-1080 cells were maintained with addition of 1% non-essential amino acids (Sigma M7145). Morphology of all cell lines was regularly checked for conformity with ATCC's specifications.

The tamoxifen-inducible *Gpx4-/-* immortalized mouse fibroblast (MF) cell line was previously described [2]. 293T, A-431, A549, HCC827, HeLa, Hep G2, HFF-1, HT-1080, LoVo, MCF 10A, MCF-7, MDA-MB-231 (MDA231), NCI-H1299 (H1299), NCI-H1437 (H1437), NCI-H1563 (H1563), NCI-H1975 (H1975), NCI-H661 (H661), PC-3, PC-9, SH-SY5Y, T-47D, U-138 MG (U138MG) and U-2 OS cell lines were purchased from ATCC. 786-O, A-498, AU565, Caki-1 and DU4475 were obtained from the Institute for Cancer Genetics, Columbia University. BJAB, HAT, HBL-1 [Human diffuse large B-cell lymphoma], Jurkat clone E6-1, OCI-Ly3, RI-1, SU-DHL-2 (SUDHL2), SU-DHL-4 (SUDHL4), SU-DHL-6 (SUDHL6), TMD8 and U-2932 cell lines were a gift from Daniel Krappmann. Co-115, HCT 116 and HT-29 cell lines were a gift from Martin Göttlicher. KBM-7 cells were a gift from Brent Cochran and spontaneously diploidized.

Chemicals

Imidazole ketone erastin (IKE), (1S,3R)-RSL3 and ferrostatin-1 (Fer-1) were synthesized by the Stockwell lab. Other chemicals and materials were obtained from commercial suppliers (Tetrahydrobiopterin dichloride (BH_4), Santa Cruz Biotechnology sc-200345; 7,8-Dihydro-L-biopterin (BH_2), Sigma 37272; TNF Recombinant Mouse Protein (TNFα), Life Technologies PMC3014; Doxorubicin hydrochloride (Doxo), Sigma PMC3014; Lipopolysaccharides (LPS), Sigma L4391; Z-VAD-FMK (zVAD), Bio-Cat T6013; Etoposide (Etop), Cayman Chemical Company 12092-100, Colchicine (Colch), Cayman Chemical Company 9000760; (±)-α-Tocopherol (αToc), Sigma T3251; Diphenyleneiodonium chloride (DPI), Enzo BML-CN240-0010); 4-Nitrobenzoic Acid (4-NB), Sigma 72910.

Generation of screening cell line MF-dCas9-MS2 and library screening

Conditional *Gpx4-/-* immortalized mouse fibroblasts (MF) were used for CRISPRa screen following infection with helper lentiviruses containing dCAS9-VP64_Blast (Addgene plasmid # 61425) and helper protein MS2-P65-HSF1_Hygro (Addgene plasmid # 61426) [1]. Viruses were made with third generation ecotropic packaging. Resistant cells were constantly selected with

additional 10 µg/mL Blasticidine S hydrochloride (Sigma 15205) and 250 µg/mL Hygromycin B (Sigma H0654).

The SAM library (Addgene # 1000000075) [3] was amplified and prepared according to instructions. Virus was produced using third generation ecotropic packaging. $1.5x10^7$ cells of the MF-dCas9-MS2 screening cell line were infected with 50 mL of supernatant containing 300,000 cfu/mL of virus particles for three days. For screening, $2.5x10^6$ cells in total were seeded in five 10-cm dishes per condition the day before. Screening conditions were 0.3 µM RSL3, 2 µM IKE and DMSO control each for 24 h. Conditional *Gpx4* knockout was induced by 1 µM (Z)-4-Hydroxytamoxifen (Sigma H7904) for 72 h in eight 10-cm dishes to ensure enough viable cells for sequencing. After ten days recovery, cells were lysed and genomic DNA was isolated by standard phenol/chloroform extraction. Samples of distinct conditions were PCR amplified and sequenced at PrimBio with primers listed in Table S5.

Screen analyses

CRISPR overexpression data deconvolution and statistical analysis was performed utilizing ENCoRE software as described previously [4]. Gene Ontology (GO) term analysis was performed on top identified genes from each condition in Figure 1A cumulatively using GSEA [5]. Genes with $\log_2$ fold changes greater than 1.0 and FDR (Bonferroni) corrected *p*-values less than 0.05 were subjected to Ingenuity Pathway Analysis (IPA, Ingenuity Systems, www.Ingenuity.com). The input genes were mapped with IPA's database, and the relevant biological pathways regulated by ferroptosis inducers were identified.

Generation of cell lines

CRISPRa overexpressing MF cell lines

To generate cell lines overexpressing individual genes, the respective guides (see Table S4) were cloned into lenti-sgRNA(MS2)_Zeo (Addgene plasmid # 61427) [1] with the selection marker changed to neomycin resistance. Empty lentiviral vector was used for the corresponding control cell line. Viruses were made using third generation ecotropic packaging. Cell pools were selected for eight days with 1 mg/mL G418 Sulfate (Geneticin Selective Antibiotic, Thermo Fisher Scientific 10131027). All lines were individually validated for survival against the three inducers from the screen and doxorubicin control as well as lipid and cytosolic ROS using BODIPY-C11 and DCF after 0.3 µM RSL3 induction for 2 h.

CRISPRi mediated knockdown cell lines

Knockdown of human *GCH1* was accomplished by cloning three guides individually (see Table S4) into pLV hU6-sgRNA hUbC-dCas9-KRAB-T2a-Puro (Addgene plasmid # 71236) [6]. For murine *Gch1* knockdown, the corresponding screening guide was used in the same vector with substituted antibiotic resistance gene (neomycin). Human cells were transiently transfected with murine mCAT1 receptor expression construct using Lipofectamine 2000 (Thermo Fisher Scientific 11668027) and subsequently infected with third generation ecotropic lentivirus

containing a pool of all three guides. Colonies were picked after corresponding antibiotic selection. Murine cells were infected accordingly and selected as pool. Cells were validated in viability assays against ferroptosis inducers and decreased mRNA levels were verified by qPCR.

Human GCH1 overexpressing HT-1080 cell line

Human GCH1 was amplified from 293T cDNA (primers see Table S5) and cloned into pCAG-IRES-Puro expression construct. The linearized construct was transfected using Lipofectamine 2000 (Thermo Fisher Scientific) at a ratio of 1:3 (DNA:reagent) into parental HT-1080 cells. Colonies were picked after 1 µg/mL Puromycin dihydrochloride (Sigma P9620) selection and clonal cell lines were validated in viability assays against ferroptosis inducers. Stable, increased *GCH1* mRNA levels were verified by qPCR.

Lentiviral transduction

Third generation ecotropic lentiviruses were made using pHCMV-EcoEnv (Addgene plasmid # 15802) [7], pRSV-Rev (Addgene plasmid # 12253) [8] and pMDLg/pRRE (Addgene plasmid # 12251) [8] and the respective transfer vectors. 293T cells were used for virus production. Cells were seeded the day before to reach 70% confluency and transfected with vector DNA mixed with XtremeGENE HP (Roche 6366244001) DNA transfection reagent in a ratio of 1:3 (DNA:reagent). Supernatant containing viral particles was collected after 72 h, filtered through a 0.45 µM syringe filter and added to recipient cells. After 48 h of infection, antibiotic selection was started to generate either pools or clones.

Cell viability assays

If not stated otherwise, cells were seeded in 96-well plates and treated overnight with the respective compounds as indicated in figures and legends. *Gpx4-/-* was induced by 1 µM 4-Hydroxytamoxifen over 72h. For BH_4 and BH_2 dose response curves, serial dilutions of both were prepared in 100 µL medium per well. 2,000 MF or HT-1080 cells were added on top containing ferroptosis inducers and incubated overnight.

Viability was assessed by adding AquaBluer (MultiTarget Pharmaceuticals 6015) according to the manufacturer's instructions and fluorescence was measured at 540 nm excitation / emission 590 nm in an Envision 2104 Multilabel plate reader (PerkinElmer). Wells were visually inspected to ensure conformity with the readout. Viability is reported as percentage relative to respective control treatment and averaged on at least two wells per condition.

High throughput cell line dose-response curves

For the cancer cell line panel in 384-well plates (Figures 5A, 5B and Figure S6), 500 cells per well were seeded in a total volume of 50 µL medium. Test compounds were prepared in at least 10-point dilution series, dissolved in DMSO alone or DMSO supplemented with 100x ferroptosis inhibitor (as indicated). The dilution series was used as 100x stock plate. The next day, 0.5 µL

from the 100x stock plate was added to the cells using automated liquid handling (i.e. 1:100 dilution). Cell viability was measured after 18 h to 22 h using AquaBluer (see above).
For other 384-well plate assays testing between multiple cell types (Figures 1C, 5F, 6F), 1,500 human cancer cells/well were seeded in 36 µL medium. Test compounds were prepared in a 16-point dilution in a mother plate dissolved in DMSO or DMSO supplemented. Compounds in the mother plate were prepared at 250x the concentration of treatment used for the cells. On the day of treatment, 3 µL from the mother plate were transferred to 72 µL of medium in a daughter plate via Biomek. 4 µL from the daughter plate was then transferred by Biomek to the cell plates. Cell viability was measured after 24 h to 26 h using CellTiter-Glo 2.0 (Promega). Cell viability in both approaches is reported as a percentage relative to the DMSO treatment.

siRNA knockdown

$1.5x10^5$ human cancer cells were seeded into six well plates in antibiotic free media. The following day, the cells were transfected with Lipofectamine RNAiMAX Transfection Reagent (Thermo Fisher Scientific 13778030) according to the manufacturer's protocol and 25pmol of siRNA (SMARTpool: ON-TARGETplus Human GCH1 siRNA, Dharmacon L-010328-00-0005 and Silencer Select Negative Control No. 2 siRNA, Thermo Fisher Scientific 4390846). After 48 h, cells were transfected again under the same conditions. The following day, cells were re-seeded at 1,500 cells/well in a white opaque bottom 384-well plate. Plates were treated with ferroptosis inducers the day after reseeding and viability was measured using CellTiter-Glo 2.0 (Promega) 36 h after treatment.

Treatment of cells with phospholipids

Lipids were purchased from Avanti Lipids as 10 mg/mL solutions in chloroform (20:4 (Cis) PC 850397, 18:0-20:4 PC 850469, 18:0-22:6 PC 850472C, 22:6 (cis) PG 840492C). Chloroform was evaporated under vacuum for 20 min and lipids were reconstituted as ethanol stocks. A 200 µM stock of each lipid in 20% 2-hydroxypropyl-beta-cyclodextrin (Cayman 16169) in PBS solution was prepared. Stocks were incubated at 37°C for 30 min and then sonicated at room temperature for 30 min until solutions were clear. 25,000 cells/well were seeded in 24-well plate. After 24 h, cells were treated with the diluted lipid solutions or vehicle. Three hours after the additions of phospholipids, cells were treated with either DMSO or 8 µM IKE. Cell viability was tested 12 h after treatment with IKE using CellTiter-Glo 2.0 Assay (Promega) according to manufacturer's protocol on a VICTOR X Multilabel Plate Reader (PerkinElmer). Cell viability is reported as a percentage relative to the DMSO treatment.

CoQ_{10} depletion

500,000 cells were seeded in a 10 cm dish per sample. CoQ_{10} was removed from the fetal bovine serum through filtration in 100 MWCO Amicon filters spun at 4,000 rpm for 30 min twice. Cells in CoQ_{10} depleted medium were treated with 1 mM 4-Nitrobenzoic acid (4-NB). Depleted

medium supplemented with 4-NB was added to cells every two days for a total of six days of treatment. On the sixth day of treatment, samples were either collected for MS analysis or treated with 6 mg/L of holo-Transferrin (Sigma T0665) along with 8 µM IKE or DMSO. Viability was tested 8 h after treatment with IKE using CellTiter-Glo 2.0 Assay (Promega) according to manufacturer's protocol on a VICTOR X Multilabel Plate Reader (PerkinElmer). Cell viability is reported as a percentage relative to the DMSO treatment. $2x10^6$ cells were collected for mass spectrometry analysis. The collected cell pellets were resuspended in 200 µL cold PBS and were lysed using a mirco-tip homogenizer. 600 µL of pre-chilled hexane/2-propanol (7:3, v/v) containing antioxidant (0.1% butylated hydroxytoluene, BHT) were added to each sample, vortexed for 30 seconds, and then incubated on ice for 20-25 min to enhance extraction efficiency of CoQ_{10}. Finally, samples were centrifuged for 25 min at 3,500 rpm at 4 °C to achieve phase separation. The organic layers were collected in a new glass vial and dried under N_2 gas. The dried samples were re-suspended in 100 µL of 2-propanol/MeCN/H_2O (55:40:5; v/v/v) containing 0.01% BHT before LC-MS analysis.

Quantitative PCR

$1x10^6$ cells per sample were trypsinized and RNA was isolated with the InviTrap Spin Universal RNA Mini Kit (Stratec Molecular 1060100200) according to the manufacturer's instructions including a DNAse treatment step (Promega M6201). Subsequently, 2 µg total RNA was reverse transcribed using RevertAid First Strand cDNA Synthesis Kit (Thermo Fisher Scientific K1622). Quantitative PCR reactions were performed using the LightCycler480 (Roche) with Power SYBR Green PCR Master Mix (Thermo Fisher Scientific 4368577) or LightCycler 480 SYBR Green I Master (Roche 04 707 516 001). Differences in mRNA levels compared to control were calculated using the ΔΔCp method relative to reference genes *Gapdh* and *Actin* for mouse and *RPL27* or *TBP* for human samples. qPCR primers are listed in Table S5.

Western blotting

Approximately $5x10^6$ cells per condition were lysed in 300 µL lysis buffer (20 mM HEPES, 350 mM NaCl, 1 mM $MgCl_2$, 0.5 mM EDTA, 0.1 mM EGTA, 20% glycine, 1% NP-40, 10 mM NaF, 1 mM DTT, 8 mM β-glycerophosphate and protease inhibitor tablet (Roche)) for 30 min. DNA was shredded with a 0.45-gauge needle and was pelleted for 20 min at maximum speed centrifugation at 4°C. The supernatant was mixed with 4x Roti®-Load (Roth) and run on a 10% SDS-PAGE gel and transferred onto PVDF membranes using electrophoretic semi-dry western blot transfer system. Membranes were blocked with 3% bovine serum albumin (BSA) in PBS-T for 1h at room temperature and incubated in primary antibody (Mouse monoclonal anti-GFRP (D11), Santa Cruz Biotechnology sc-514098; Goat polyclonal anti-Actin (I-19), Santa Cruz Biotechnology sc-1616) diluted 1:1,000 in 1.5% BSA in PBS-T overnight at 4°C. Membranes were washed for 5 min in PBS-T before addition of HRP-coupled secondary antibodies (Donkey polyclonal anti-mouse 715-035-150 and Donkey polyclonal anti-goat 705-035-147; all Dianova)

diluted 1:7,000 in 0.75% BSA in PBS-T for 1 h at room temperature. LumiGLO Reagent (Cell Signaling) was used for chemiluminescence detection according to the manufacturer's instructions.

Detection of lipid and cytosolic ROS

Lipid and cytosolic reactive oxygen species (ROS) were detected using flow cytometry. 5,000 cells per well were seeded in 96-well plates in triplicate per condition. The next day, medium was replaced with 100 µL medium containing ferroptosis inducers. For BH_4 and BH_2 testing, cells were treated with 0.3 µM RSL3 and 50 µM BH_4 or BH_2 for 3h. For overexpression cell line validation (Figure S1C), cells were induced with 0.3 µM RSL3 for 2 h. Subsequently, fluorescence dye to a final concentration of 2 µM BODIPY 581/591 C11 (BODIPY-C11, Thermo Fisher Scientific D3861) for lipid ROS or 25 µM 2,7-Dichlorodihydrofluorescein diacetate (DCF, Cayman Chemical 85155) for cytosolic ROS were added on top and cells were incubated for another 30 min. After removal of the medium, wells were rinsed with 30 µL PBS before adding 30 µL Accutase (Sigma A6964) to each well. Detached cells were resuspended in 170 µL PBS per well followed by analysis on an Attune acoustic flow cytometer (Applied Biosystems). 10,000 events per well were collected from the BL-1 channel (excited by 488 nm laser). The median fluorescence intensity of each well was determined and normalized to DMSO treated control cells using FlowJo 10 software.

Cell-free oxidation assay based on Bodipy-C11

All working solutions in PBS were freshly prepared at 3x of their final concentration. 150 µL ferroptosis inhibitors were prepared to achieve equal amounts of DMSO per sample (final as indicated). An equal volume of 3x BODIPY-C11 (final 0.625 µM, Thermo Fisher Scientific) was added. Oxidation was initiated by adding one volume freshly dissolved 2,2'-Azobis(2-amidinopropane) dihydrochloride (AAPH, VWR International CAYM82235-1) in PBS (final 2.5 mM). After vortexing, reaction tubes were incubated for 1 h at room temperature in the dark. 75 µL sample per well were measured in triplicate in black 384-well plates on an Envision 2104 plate reader (PerkinElmer). Fluorescence intensity of oxidized BODIPY-C11 at excitation 495 nm / emission 520 nm emission was quantified and normalized to DMSO. Mean ± SD was reported and significance was determined by unpaired t-test against DMSO.

Antioxidant assay based on electron-transfer

The assay was performed as previously described by [9]. In brief, 5 µL of 10 mM compound in DMSO were added to 1 mL of 0.05 mM 2,2-diphenyl-1-picrylhydrazyl (DPPH, Sigma D9132) in methanol and rotated for 10 min at room temperature. Using a clear bottom 96-well plate, 200 µL reaction per well were measured in quadruplicate at an absorbance of 517 nm in an Envision 2104 plate reader (PerkinElmer). Background absorption of DPPH alone was subtracted from all values.

Free thiol labelling assay

2,500 cells per well were seeded in clear-bottom 96-well plates. After 24 h, cells were treated as indicated with 25 µM tert-Butylhydroquinone (tBHQ, Alfa Aesar A19206.36) as positive control to induce GSH, 100 µM buthionine sulfoximine (BSO, Sigma B2515) as GSH-depleting negative control, 25 µM BH_4 and 25 µM BH_2 and incubated for 24 h. Medium was replaced with the same substances and 0.3 µM RSL3 was added. Cells were incubated for 3 h. For the nuclear staining and GSH labelling, medium was replaced with 100 µL pre-warmed PBS supplemented with 1 µg/mL Hoechst 33342 (Thermo Fisher Scientific H3570) and 40 µM dibromobimane (Tebu-Bio F-0040) and incubated for 30 min. Free thiol label was quantified by dibromobimane at excitation 393 nm / emission 477 nm with an Envision 2104 plate reader (PerkinElmer). For normalization to the cell number, Hoechst fluorescence was recorded at excitation 340 nm / emission 450 nm emission. Blank autofluorescence values of compounds with Hoechst and Dibromobimane were subtracted.

Sample preparation for metabolomics and proteomics

Generally, $2x10^6$ cells were seeded in five replicates per condition the day before on 10-cm dishes and treated as indicated with ferroptosis inducers on the next day. For targeted analysis of BH_4 and BH_2 in SH-SY5Y cell lines, cells were left untreated for 40 h. HT-1080 cells for targeted analysis were seeded at $4x10^5$ cells per well in six replicates in 6-well plates and left untreated overnight. Cells were detached using Accutase (Sigma A6964), resuspended in medium and pelleted at 125 g for 5 min. Then, cells were resuspended in PBS, pelleted again and snap-frozen in liquid nitrogen. Mouse fibroblast samples were prepared in one cell culture experiment for both mass spectrometric analyses and divided at a ratio of 5:1 for metabolomics and proteomics during resuspension in PBS. All samples were stored at -80°C.

Global metabolomic analysis

Cell cleavage was performed in a cooled (-3.5°C) Precellys (Bertin Instruments) using soft extraction with ceramic beads (2 repetition cycles, 15 sec) in 0.1 ml 80% methanol followed by a centrifugation step (15 min, 13,000 rpm, 4°C). 15 µL of each sample were taken and pooled for quality control. Five biological replicates were analyzed. We profiled global changes in the metabolome with two complementary mass spectrometry approaches, direct-injection electrospray ionization Fourier transform ion cyclotron resonance mass spectrometry (ESI FT/ICR-MS, 12T solariX, Bruker Daltonics) and reversed phase ultra-performance liquid chromatography (UPLC-QqToF-MS, maXis, Bruker Daltonics). Both techniques were performed in positive electrospray ionization. Ultrahigh resolution mass spectra were acquired on a 12T solariX FT/ICR-MS equipped with an Apollo II electrospray source (Bruker Daltonics). The mass spectrometer was tuned in order to obtain highest sensitivity for metabolites in the m/z range of about 150 to 600 Da in broadband detection mode with a time domain transient of 2

Megawords. The instrument was calibrated with a 1 ppm arginine solution. Acquired mass spectra were internally calibrated against a set of endogenous metabolites. A mass error below 100 ppb was achieved. Cell extracts were diluted 1:10 in methanol and injected with 120 µL/h.

FT/ICR-MS

Mass lists were generated with a signal-to-noise ratio (S/N) of four, exported, and combined to one data matrix by applying a 1 ppm window. Ions were annotated to the ionic derivatives of the metabolites listed in the KEGG database for Homo sapiens allowing 1 ppm tolerance. Not yet identified metabolites were annotated by their elemental composition using mass-differences based network approach as published [10,11].

Statistical analysis

To identify metabolites that show significant change a Mann-Whitney test with FDR significance criterion (based on Benjamini-Hochberg-correction) was performed. Global metabolome modifications were investigated using a principal component analysis (SIMCA-P) and hierarchical cluster analysis (HCE) after unit variance scaling and mean centering. To identify significant differences among metabolites between MF *Gch1* OE and control cells, we applied a supervised PLS-DA, performing 100 random permutations. The quality of the model was validated using 100 random permutations. FT/ICR-MS detected m/z values are given in Table S2.

Targeted analysis of BH_4 and derivatives

A targeted UPLC-qTOF-MS/MS (Acquity, Waters, hyphened to maXis, Bruker Daltonics) analysis for a set of BH_4 and derivatives was built up based on HILIC stationary phase (Hydrophilic interaction chromatography, iHILIC-Fusion, Hilicon AB, 100 * 2.1 mm, 1.8 µm, 100 Å). Mobile phase A consisted of acetonitrile/water (95:5, v/v), 5 mM ammonium acetate at pH 4.6 and mobile phase B of acetonitrile/water (30:70, v/v), 25 mM ammonium acetate (pH 4.6). A 4 min gradient of 70% B to 99.9% B flow rate was kept constant at 0.5 ml/min at 60°C. BH_4 identification was further supported by detection of the main fragment of m/*z* 166.07 (Figure S3C) [12].

Quantitative proteomics

Cell pellets were lysed by vortexing and sonification in two freeze-thaw cycles using 200 µL 8 M urea in 0.1 M Tris/HCl pH 8.5. Equal total protein amounts (10 µg) of the resulting crude cell lysate were digested with a modified FASP procedure [13,14] using Lys-C and trypsin as proteases and Microcon centrifugal filters (Sartorius Vivacon 500 30kDa). Approximately 0.5 µg peptides per sample were measured in a randomized fashion on a Q-Exactive HF mass spectrometer online coupled to an Ultimate 3000 RSLC (Thermo Fisher Scientific) in data-independent acquisition mode as described previously [15,16]. The recorded raw files were analyzed using the Spectronaut Pulsar software (Biognosys; [17]) with a peptide identification false discovery rate <1% , using an in-house mouse spectral library which was generated using Proteome Discoverer 2.1 and the Swissprot Mouse database (release 2016_02). Quantification was based on MS2

area levels of all unique peptides per protein and normalized protein quantifications were exported. Log_2 transformed abundance ratios to the median abundance per protein were used for heat map generation in cluster 3.0 [18], with clustering of proteins using the 'Euclidean distance' setting and the 'complete linkage' algorithm. The resulting tree and heat map were visualized with Java Treeview. The mass spectrometry proteomics data have been deposited to the ProteomeXchange Consortium via the PRIDE [19] partner repository with the dataset identifier PXD014810.

Untargeted lipidomics

$5x10^6$ cells treated with DMSO or 10 µM IKE for 6 h were homogenized using a microtip sonicator in 250 µL cold methanol containing 0.1% butylated hydroxyl toluene (BHT). Samples were transferred to glass tubes containing 850 µL of cold methyl-tert-butyl ether (MTBE) and vortexed for 30 sec. Samples were then incubated at 4 °C for 1 h on a shaker. 200 µL of cold water was added to each sample and incubated on ice for 20 min before centrifugation at 3,000 rpm for 20 min at 4 °C to enhance protein precipitation and phase separation. The organic layer containing lipids was collected and dried under a stream of nitrogen gas on ice. Next, the samples were reconstituted in a solution of 2-propanol/acetonitrile/water (4:3:1, v/v/v) containing a mixture of internal standard for LC-MS analysis. A quality control sample was prepared by combining 40 µL of each sample to assess the reproducibility of the features through the runs.

Ultra-performance liquid chromatography analysis

Chromatographic separation of extracted lipids was carried out at 55°C on Acquity UPLC CSH C18 Column, (130 Å, 1.7 µm, 2.1 mm X 100 mm; Waters) over a 20 min gradient elution. Mobile phase A consisted of acetonitrile/water (60:40, v/v) and mobile phase B was 2-propanol/acetonitrile/water (85:10:5, v/v/v) both containing 10 mM ammonium acetate and 0.1% acetic acid. After injection, the gradient was held at 40% mobile phase B for 2 min. At 2.1 min, it reached to 50% B, then increased to 70% B in 12 min, at 12.1 min changed to 70% B and at 18 min increased to 90% B. The eluent composition returned to the initial condition in 1 min, and the column was re-equilibrated for an additional 1 min before the next injection was conducted. The flow rate was set to 0.4 mL/min and injection volumes were 6 µL using the flow through needle mode in both positive and negative ionization modes.

The QC sample was injected between the samples and at the end of the run to monitor the performance and the stability of the MS platform. This QC sample was also injected at least 5 times at the beginning of the UPLC/MS run, in order to condition the column.

Mass spectrometry analysis

The Synapt G2 mass spectrometer (Waters) was operated in both positive and negative ESI modes. For positive mode, a capillary voltage and sampling cone voltage of 3 kV and 32 V were used. The source and desolvation temperature were kept at 120°C and 500°C, respectively. Nitrogen was used as desolvation gas with a flow rate of 900 L/h. For negative mode, a capillary

voltage of -2 kV and a cone voltage of 30 V were used. The source temperature was 120°C, and desolvation gas flow was set to 900 L/h. Dependent on the ionization mode the protonated molecular ion of leucine encephalin ($[M+H]^+$, m/z 556.2771) or the deprotonated molecular ion ($[M-H]^-$, m/z 554.2615) was used as a lock mass for mass accuracy and reproducibility. Leucine enkephalin was introduced to the lock mass at a concentration of 2 ng/mL (50% acetonitrile containing 0.1% formic acid), and a flow rate of 10 μL/min. The data was collected in duplicates in the centroid data independent (MS^E) mode over the mass range m/z 50 to 1600 Da with an acquisition time of 0.1 sec per scan. The QC samples were also acquired in enhanced data independent ion mobility (IMS-MS^E) in both positive and negative modes for enhancing the structural assignment of lipid species. The ESI source settings were the same as described above. The traveling wave velocity was set to 650 m/s and wave height was 40 V. The helium gas flow in the helium cell region of the ion-mobility spectrometry (IMS) cell was set to 180 mL/min to reduce the internal energy of the ions and minimize fragmentation. Nitrogen as the drift gas was held at a flow rate of 90 mL/min in the IMS cell. The low collision energy was set to 4 eV, and high collision energy was ramping from 25 to 65 eV in the transfer region of the T-Wave device to induce fragmentation of mobility-separated precursor ions.

For the measurements of both reduced and oxidized CoQ_{10}, the samples were run in similar LC-MS conditions as mentioned above except that the LC gradient was reduced to 10 min.

Data pre-processing and statistical analysis

All raw data files were converted to netCDF format using DataBridge tool implemented in MassLynx software (Waters, version 4.1). Then, they were subjected to peak-picking, retention time alignment, and grouping using XCMS package (version 3.0.2) in R (version 3.4.4) environment. For the peak picking, the CentWave algorithm was used with the peak width window of 2 to 25 s. For peak grouping, bandwidth and m/z-width of 2 s and 0.01 Da were used, respectively. After retention time alignment and filling missing peaks, an output data frame was generated containing the list of time-aligned detected features (m/*z* and retention time) and the relative signal intensity (area of the chromatographic peak) in each sample. Technical variations such as noise were assessed and removed from extracted features' list based on the ratios of average relative signal intensities of the blanks to QC samples (blank/QC >1.5). Also, peaks with variations larger than 30% in QCs were eliminated. All the extracted features were normalized to measured protein concentrations measured by BCA assay. Statistical analyses were performed in MetaboAnalyst (version 4.0) and Heatmaps were generated in R (version 3.4.4). Group differences were calculated using one-way ANOVA (Post-hoc Fisher's LSD, $p < 0.05$) and false discovery rate of 5% to control for multiple comparisons.

Structural assignment of identified lipids

Identification and structural characterization of significant lipid features were initially obtained by searching monoisotopic masses against the available online databases such as METLIN, Lipid MAPS, and HMDB with a mass tolerance of 5 ppm. Fragment ion information obtained by tandem MS (UPLC-$HDMS^E$) was utilized for further structural elucidation of significantly changed

lipid species (Table S3). All lipid annotations follow the "Comprehensive Classification System for Lipids" developed by the International Lipid Classification and Nomenclature Committee [20,21]. HDMSE data were processed using MS^E data viewer (Version 1.3, Waters, MA, USA).

Cell extrinsic medium test

Donor cell lines were seeded at the respective numbers on 10-cm dishes in 5mL medium. After 24 h, the conditioned medium was harvested and cells were briefly spun down. When indicated, medium was supplemented with 2 µM IKE for ferroptosis induction with or without 10 µM α-Tocopherol (αToc) as rescue control before adding to 3,000 parental HT-1080 recipient cells that were seeded in a 96-well plate the day before. Viability was normalized to each medium condition's DMSO control. Significance was determined by an unpaired t-test.

Generation of three-dimensional spheroids and IKE treatment

3D-spheroids were formed by seeding 500 parental HT-1080 or *GCH1* OE cells per well into the GravityTRAP ULA 96-well plates (InSphero/PerkinElmer). 3D spheroids showed low interwell variations below 10% and were matured for 5 days, followed by treatment with 2 µM IKE for additional 48h and 1 h staining using Hoechst 33342. 3D-spheroids were analyzed directly in ultralow attachment assay plates with an Operetta High Content Imaging System (PerkinElmer) without additional pipetting steps during assay analysis. Images from a single plate were acquired using Brightfield and Hoechst 33342 (blue) channels and 10x High-NA objective in wide field mode.

Differentially expressed gene (DEG) analysis

TCGA RNA-seq datasets were downloaded by UCSC Xena browser (https://xenabrowser.net/). Statistical analysis was performed using R/Bioconductor (R: A language and environment for statistical computing. R Version: 3.5. R Foundation for Statistical Computing, Vienna, Austria. URL http://www.R-project.org/). DEG analysis was performed by the Limma package [22]. The tissues were separated into normal and tumour tissues. An empirical Bayesian approach was applied to estimate the gene expression changes using moderated t-tests in BRCA, KICH, KIRC and KIRP tissues. The adjusted *p*-value for multiple testing was calculated using the Benjamini-Hochberg correction.

Statistics

Generally, statistical analyses were performed in GraphPad Prism. All cell viability results are reported as mean ± SEM of at least two technical replicates. In cell-free assays and targeted metabolomic data mean ± SD is shown. Individual experiments were repeated independently at least three times on different days with similar results and a representative experiment is shown. If not stated otherwise, significance was determined using Student's unpaired t-test against respective control conditions (* $p < 0.05$; ** $p < 0.01$; *** $p < 0.001$; ns = not significant).

SUPPORTING REFERENCES

(1) Konermann, S.; Brigham, M. D.; Trevino, A. E.; Joung, J.; Abudayyeh, O. O.; Barcena, C.; Hsu, P. D.; Habib, N.; Gootenberg, J. S.; Nishimasu, H.et al. Genome-scale transcriptional activation by an engineered CRISPR-Cas9 complex. *Nature* **2015,** *517* (7536), 583.

(2) Mannes, A. M.; Seiler, A.; Bosello, V.; Maiorino, M.; Conrad, M. Cysteine mutant of mammalian GPx4 rescues cell death induced by disruption of the wild-type selenoenzyme. *FASEB J* **2011,** *25* (7), 2135.

(3) Joung, J.; Konermann, S.; Gootenberg, J. S.; Abudayyeh, O. O.; Platt, R. J.; Brigham, M. D.; Sanjana, N. E.; Zhang, F. Genome-scale CRISPR-Cas9 knockout and transcriptional activation screening. *Nature protocols* **2017,** *12* (4), 828.

(4) Trumbach, D.; Pfeiffer, S.; Poppe, M.; Scherb, H.; Doll, S.; Wurst, W.; Schick, J. A. ENCoRE: an efficient software for CRISPR screens identifies new players in extrinsic apoptosis. *BMC genomics* **2017,** *18* (1), 905.

(5) Qi, L. S.; Larson, M. H.; Gilbert, L. A.; Doudna, J. A.; Weissman, J. S.; Arkin, A. P.; Lim, W. A. Repurposing CRISPR as an RNA-guided platform for sequence-specific control of gene expression. *Cell* **2013,** *152* (5), 1173.

(6) Thakore, P. I.; D'Ippolito, A. M.; Song, L.; Safi, A.; Shivakumar, N. K.; Kabadi, A. M.; Reddy, T. E.; Crawford, G. E.; Gersbach, C. A. Highly specific epigenome editing by CRISPR-Cas9 repressors for silencing of distal regulatory elements. *Nat Methods* **2015,** *12* (12), 1143.

(7) Sena-Esteves, M.; Tebbets, J. C.; Steffens, S.; Crombleholme, T.; Flake, A. W. Optimized large-scale production of high titer lentivirus vector pseudotypes. *Journal of virological methods* **2004,** *122* (2), 131.

(8) Dull, T.; Zufferey, R.; Kelly, M.; Mandel, R. J.; Nguyen, M.; Trono, D.; Naldini, L. A third-generation lentivirus vector with a conditional packaging system. *Journal of virology* **1998,** *72* (11), 8463.

(9) Dixon, S. J.; Lemberg, K. M.; Lamprecht, M. R.; Skouta, R.; Zaitsev, E. M.; Gleason, C. E.; Patel, D. N.; Bauer, A. J.; Cantley, A. M.; Yang, W. S.et al. Ferroptosis: an iron-dependent form of nonapoptotic cell death. *Cell* **2012,** *149* (5), 1060.

(10) Muller, C.; Dietz, I.; Tziotis, D.; Moritz, F.; Rupp, J.; Schmitt-Kopplin, P. Molecular cartography in acute Chlamydia pneumoniae infections--a non-targeted metabolomics approach. *Analytical and bioanalytical chemistry* **2013,** *405* (15), 5119.

(11) Tziotis, D.; Hertkorn, N.; Schmitt-Kopplin, P. Kendrick-analogous network visualisation of ion cyclotron resonance Fourier transform mass spectra: improved options for the assignment of elemental compositions and the classification of organic molecular complexity. *European journal of mass spectrometry (Chichester, England)* **2011,** *17* (4), 415.

(12) Fismen, L.; Eide, T.; Djurhuus, R.; Svardal, A. M. Simultaneous quantification of tetrahydrobiopterin, dihydrobiopterin, and biopterin by liquid chromatography coupled electrospray tandem mass spectrometry. *Analytical biochemistry* **2012,** *430* (2), 163.

(13) Grosche, A.; Hauser, A.; Lepper, M. F.; Mayo, R.; von Toerne, C.; Merl-Pham, J.; Hauck, S. M. The Proteome of Native Adult Muller Glial Cells From Murine Retina. *Mol Cell Proteomics* **2016,** *15* (2), 462.

(14) Wisniewski, J. R.; Zougman, A.; Nagaraj, N.; Mann, M. Universal sample preparation method for proteome analysis. *Nat Methods* **2009,** *6* (5), 359.

(15) Lepper, M. F.; Ohmayer, U.; von Toerne, C.; Maison, N.; Ziegler, A. G.; Hauck, S. M. Proteomic Landscape of Patient-Derived CD4+ T Cells in Recent-Onset Type 1 Diabetes. *J Proteome Res* **2018,** *17* (1), 618.

(16) Mattugini, N.; Merl-Pham, J.; Petrozziello, E.; Schindler, L.; Bernhagen, J.; Hauck, S. M.; Gotz, M. Influence of white matter injury on gray matter reactive gliosis upon stab wound in the adult murine cerebral cortex. *Glia* **2018**, DOI:10.1002/glia.23329 10.1002/glia.23329.

(17) Bruderer, R.; Bernhardt, O. M.; Gandhi, T.; Reiter, L. High-precision iRT prediction in the targeted analysis of data-independent acquisition and its impact on identification and quantitation. *Proteomics* **2016,** *16* (15-16), 2246.

(18) Eisen, M. B.; Spellman, P. T.; Brown, P. O.; Botstein, D. Cluster analysis and display of genome-wide expression patterns. *Proceedings of the National Academy of Sciences of the United States of America* **1998,** *95* (25), 14863.

(19) Perez-Riverol, Y.; Csordas, A.; Bai, J.; Bernal-Llinares, M.; Hewapathirana, S.; Kundu, D. J.; Inuganti, A.; Griss, J.; Mayer, G.; Eisenacher, M.et al. The PRIDE database and related tools and resources in 2019: improving support for quantification data. *Nucleic Acids Res* **2019,** *47* (D1), D442.

(20) Fahy, E.; Subramaniam, S.; Murphy, R. C.; Nishijima, M.; Raetz, C. R.; Shimizu, T.; Spener, F.; van Meer, G.; Wakelam, M. J.; Dennis, E. A. Update of the LIPID MAPS comprehensive classification system for lipids. *Journal of lipid research* **2009,** *50 Suppl*, S9.

(21) Liebisch, G.; Vizcaino, J. A.; Kofeler, H.; Trotzmuller, M.; Griffiths, W. J.; Schmitz, G.; Spener, F.; Wakelam, M. J. Shorthand notation for lipid structures derived from mass spectrometry. *Journal of lipid research* **2013,** *54* (6), 1523.

(22) Smyth, G. K. In *Bioinformatics and Computational Biology Solutions Using R and Bioconductor*; Gentleman, R.;Carey, V. J.;Huber, W.;Irizarry, R. A.;Dudoit, S., Eds.; Springer New York: New York, NY, 2005, DOI:10.1007/0-387-29362-0_23 10.1007/0-387-29362-0_23.